Molecular Catalysis 442 (2017) 74–82

Contents lists available at ScienceDirect

Molecular Catalysis

journal homepage: www.elsevier.com/locate/mcat

MCAT

Selective reduction of NO over Cu/Al_2O_3: Enhanced catalytic activity by infinitesimal loading of Rh on Cu/Al_2O_3

Saburo Hosokawa[a,b,*], Kazuya Matsuki[b], Kyoko Tamaru[b], Yudai Oshino[b], Hirofumi Aritani[c], Hiroyuki Asakura[a,b], Kentaro Teramura[a,b], Tsunehiro Tanaka[a,b,*]

[a] Elements Strategy Initiative for Catalysts & Batteries (ESICB), Kyoto University, Kyotodaigaku Katsura, Nishikyo-ku, Kyoto 615-8245, Japan
[b] Department of Molecular Engineering, Graduate School of Engineering, Kyoto University, Kyotodaigaku Katsura, Nishikyo-ku, Kyoto 615-8510, Japan
[c] Department of Life Science and Green Chemistry, Saitama Institute of Technology, 1690 Fusaiji, Fukaya, Saitama 369-0293, Japan

ARTICLE INFO

Article history:
Received 24 July 2017
Received in revised form 30 August 2017
Accepted 4 September 2017

Keywords:
Selective reduction of NO
Cu/Al_2O_3
Precious metal loading

ABSTRACT

This study demonstrates that an isolated Cu^{2+} species formed by interacting with tetrahedral Al species on γ-Al_2O_3 shows a high catalytic activity for NO reduction with C_3H_6 and CO under high oxygen concentrations (lean conditions), and that an infinitesimal amount of Rh (0.01 wt%, 100 ppm) loaded on 0.5 wt% Cu/Al_2O_3 is a more effective catalyst for the reactions, under a wide range of oxygen concentrations, than 0.5 wt% Pd/Al_2O_3 or 1.0 wt% Rh/Al_2O_3. Although 0.5 wt% Cu/Al_2O_3 itself is effective for the reaction at lean conditions, it shows low catalytic activity under stoichiometric and low oxygen concentrations (rich conditions). On the other hand, the loading of 0.01 wt% Rh on Cu/Al_2O_3 dramatically improves catalytic activities under stoichiometric and rich conditions, with maintaining the high NO reduction activity of Cu/Al_2O_3 itself under lean conditions. Therefore, a Rh species in the $Rh/Cu/Al_2O_3$ system must play a role as an active site under stoichiometric and rich conditions. Under lean conditions using $Rh/Cu/Al_2O_3$, an isolated Cu^{2+} species on γ-Al_2O_3 mainly contributes to the NO reduction properties of the catalyst. No such advantage was observed for $Pd/Cu/Al_2O_3$; that is, the catalytic activity of Cu/Al_2O_3 under lean conditions is diminished by Pd loading. Hence, we reveal that the roles of the Rh and Cu species in the Rh-loaded Cu/Al_2O_3 catalyst are effectively shared according to oxygen concentration in selective reduction of NO, when loaded with an infinitesimal amount of Rh. These observations provide novel guidelines for the development of catalysts that more beneficially use precious metal resources.

1. Introduction

Nitrogen oxides (NO_x) emitted from various sources, including mobile sources such as automobiles and aircraft, and stationary sources such as factories and homes, are well known to have serious effects as air pollutants on global environmental problems. Typical nitrogen oxides are nitric oxide (NO), nitrogen dioxide (NO_2) and nitrous oxide (N_2O). Nitric oxide (NO) and nitrogen dioxide (NO_2) cause acid rain and photochemical smog, while N_2O deteriorates the ozone layer [1]. Among them, a large amount of NO_x has been exhausted from automobiles [2]. Consequently, the selective reduction of NO_x from automotive engines to N_2 has been a longstanding challenge [3].

To date, NO_x-containing pollutants emitted from gasoline engines in automobiles have been purified by a three-way catalytic system that mainly removes the three harmful components: NO, carbon monoxide (CO), and hydrocarbons (HCs) [4]. Since the regulations controlling exhaust gases become more restrictive from year to year, increasingly large amounts of platinum-group-metal species (PGMs), such as Pd, Rh and Pt, are being used in these catalytic systems [5–12]. From an economic perspective, novel catalysts for the purification of exhaust gases that use lower amounts of precious metals, or other alternatives, are highly desired and their development has been actively pursued. To that end, many studies into selective reductions of NO using base-metal catalysts have been reported recently [13–20].

The concentration of oxygen in automobile exhaust gases is a very important factor for selective reduction of NO. HCs and CO are oxidized by air to form CO_2 and H_2O, but NO must be completely reduced to N_2 despite the presence of oxygen. In other

* Corresponding authors at: Elements Strategy Initiative for Catalysts & Batteries (ESICB), Kyoto University, Kyotodaigaku Katsura, Nishikyo-ku, Kyoto 615-8245, Japan.
E-mail addresses: hosokawa@moleng.kyoto-u.ac.jp (S. Hosokawa), tanakat@moleng.kyoto-u.ac.jp (T. Tanaka).

http://dx.doi.org/10.1016/j.mcat.2017.09.005
2468-8231/

words, purification efficiency depends on the air-to-fuel ratio (A/F) [21–23]; in low A/F ratios, HCs and CO cannot be completely oxidized, whereas in high A/F ratios the reduction of NO becomes difficult. As a consequence, all pollutants are usually purified under stoichiometric conditions, where the A/F is around 14.6, over PGM-containing catalysts. Considering the variations in A/F that are associated with different driving modes, improved catalyst materials, that are applicable over a wide range of oxygen concentrations, are highly desired.

With this background in mind, the development of Cu-based systems as effective catalysts for selective reductions of NO has been a focus for many years [24–30]. For example, Cu^{2+} ion-exchange zeolites and Cu/Al_2O_3 have been reported to show high catalytic activities for NO reduction and are viewed as alternatives to noble metals [31–36]. We have also shown that highly dispersed Cu^{2+} species on catalyst supports contribute to the catalytic activity of NO-CO reactions under an oxygen-rich atmosphere [37]; hence, highly dispersed Cu species impacts positively on selective reduction of NO.

The present study investigated NO reductions during NO-CO-C_3H_6 reactions, over Cu/Al_2O_3-based catalysts, under a variety of oxygen concentrations. Herein, we reveal that an isolated Cu^{2+} species, which strongly interacts with the tetrahedral Al species in γ-Al_2O_3, shows high catalytic activity for NO reductions under slightly lean conditions. We also demonstrate for the first time that an infinitesimal loading (100 ppm) of Rh on Cu/Al_2O_3 dramatically improves catalytic activity over a wide range of oxygen concentrations.

2. Experimental methods

2.1. Catalyst preparation

γ-Al_2O_3 (JRC-ALO-4; 177 $m^2\,g^{-1}$) and CeO_2 (JRC-CEO-3; 92 $m^2\,g^{-1}$) were provided by the Catalysis Society of Japan. ZrO_2 (z-2965; 66 $m^2\,g^{-1}$) was kindly provided by the Daiichi Kigenso Kogyo Co., Ltd. Cu-loaded catalysts were prepared using an impregnation method. In the case of 0.5 wt% Cu-loaded catalyst, a Cu aqueous solution (1.58×10^{-2} mol L^{-1}) was prepared by dissolving $Cu(NO_3)_2{\cdot}3H_2O$. The support (0.995 g) was added to the mixture of a deionized water (3 mL) and the Cu solution (5 mL), followed by solvent evaporation at 80 °C. The resulting powder was calcined in air at 773 K for 5 h.

PGM/Cu/Al_2O_3 catalysts were prepared by a gradual impregnation method in which 0.5 wt% Cu/Al_2O_3 was added to an aqueous solution containing $Pt(NH_3)_2(NO_2)_2$, or an ethyl acetate solution containing $Pd(OAc)_2$ or $Rh(acac)_3$. For example, 0.01 wt% Rh/0.5 wt% Cu/Al_2O_3 catalyst was synthesized as follows. A Rh ethylacetate solution (1.00×10^{-3} mol L^{-1}) was prepared by dissolving $Rh(acac)_3$. 0.5 wt% Cu/Al_2O_3 (0.999 g) obtained by calcination at 773 K was added to the mixture of acetone (8 mL) and the Rh solution (1 mL), followed by solvent evaporation at room temperature. The resulting powder was calcined in air at 773 K for 5 h.

The BET surface areas of representative catalysts were summarized in Table S1.

2.2. Catalytic reactions

Catalytic experiments were carried out in a fixed-bed flow reactor at atmospheric pressure. A 200 mg sample of the catalyst (25/50 mesh) was placed in a tubular reactor. The reaction gas (100 mL min^{-1}), composed of 1000 ppm NO, 1000 ppm CO, 250 ppm C_3H_6, 0–2812.5 ppm O_2, and He as the balance, was introduced to the catalyst bed at $W/F = 0.12$ g s mL^{-1} (gas hourly space velocity, GHSV ≈ 15000 h^{-1}). Before each experiment, the catalyst was heated to 773 K in a stream of He for 1 h. The effluent gases from the reactor were analyzed by gas chromatography (Shimadzu GC-8A, Porapak Q and MS-5A columns) equipped with a thermal conductivity (TC) detector.

The λ value was used as an indicator of oxygen concentration and was calculated according to the following equation:

$$\lambda = ([CO]_a + [NO]_a + [O_2]_a \times 2)/([CO]_s + [NO]_s + [O_2]_s \times 2)$$

$[CO]_a$, $[NO]_a$, and $[O_2]_a$ represent the actual gas concentrations, and $[CO]_s$, $[NO]_s$, and $[O_2]_s$ are the concentrations under stoichiometric condition.

Under the reaction condition described above, the concentrations of CO, C_3H_6 and NO were fixed, and $[O_2]$ was varied from 2812.5 ppm to 0 ppm. The chemical reaction equation under stoichiometric condition is:

$$CO + C_3H_6 + 4\,NO + 9/2\,O_2 \rightarrow 2\,N_2 + 7\,CO_2 + 3\,H_2O$$

Therefore, the oxygen concentration corresponding to $\lambda = 1$, $[O_2]_s$, is 1125 ppm, and the λ value in the catalytic reaction ranged from 1.79 to 0.47. A λ value of 1 is considered to correspond to A/F = 14.6. The outlet gases were analyzed after the reaction at each oxygen concentration had proceeded for 30 min.

Catalytic CO oxidation experiments were also performed in a fixed-bed reactor as described above. The reaction gas (100 mL min^{-1}), composed of 1000 ppm CO, 1000 ppm O_2, and He as the balance, was introduced to the catalyst (200 mg) at $W/F = 0.12$ g s mL^{-1}. The reaction gas for C_3H_6 oxidation experiments was composed of 250 ppm C_3H_6, and 2250 ppm O_2, with He as the balance.

2.3. Characterizations

X-ray diffraction (XRD) measurements were performed on a Rigaku Ultima IV X-ray diffractometer with Cu-Kα radiation. The Al K-edge X-ray absorption fine structure (XAFS) spectra were recorded in total-electron-yield mode at room temperature by using a InSb double-crystal monochromator at the UVSOR-IMR BL2A beamline. Cu K-edge XAFS spectra were measured on the SPring-8 BL01B1 beamline, and were recorded in transmission mode at room temperature using a Si(111) double-crystal monochromator. X-ray photoelectron spectroscopy (XPS) spectra were recorded on a Shimadzu ESCA using Mg-Kα radiation. Electron spin resonance (ESR) spectra were recorded at room temperature on a JEOL JES-X320 ESR spectrometer with the following settings: center field, 300 mT; sweep width, ±7 mT; modulation width, 1.0×0.1 mT; amplitude, 5 mT; and time constant, 0.03 s. The catalysts were treated at room temperature for 1 h under vacuum, before ESR measurements. Diffuse reflectance infrared Fourier transform (DRIFT) spectra were acquired on an FT/IR-4700 spectrometer (JASCO, Japan), equipped with a mercury-cadmium-tellurium (MCT) detector cooled by liquid N_2. The catalyst was pre-treated with He (100 mL min^{-1}) at 773 K for 1 h and the spectrum of the sample treated in this manner was used as the background. The reaction gas corresponding to a lean condition (total flow rate, 100 mL min^{-1}: NO, 1000 ppm; C_3H_6, 250 ppm; O_2, 2250 ppm; He balance) was then introduced into the cell. DRIFT spectra were obtained after the reaction had proceeded for 30 min at 773 K.

3. Results and discussion

3.1. Catalyst characterizations

Cu/Al_2O_3 catalysts were prepared by impregnation of γ-Al_2O_3 with an aqueous solution containing $Cu(NO_3)_2{\cdot}3H_2O$ at 353 K, fol-

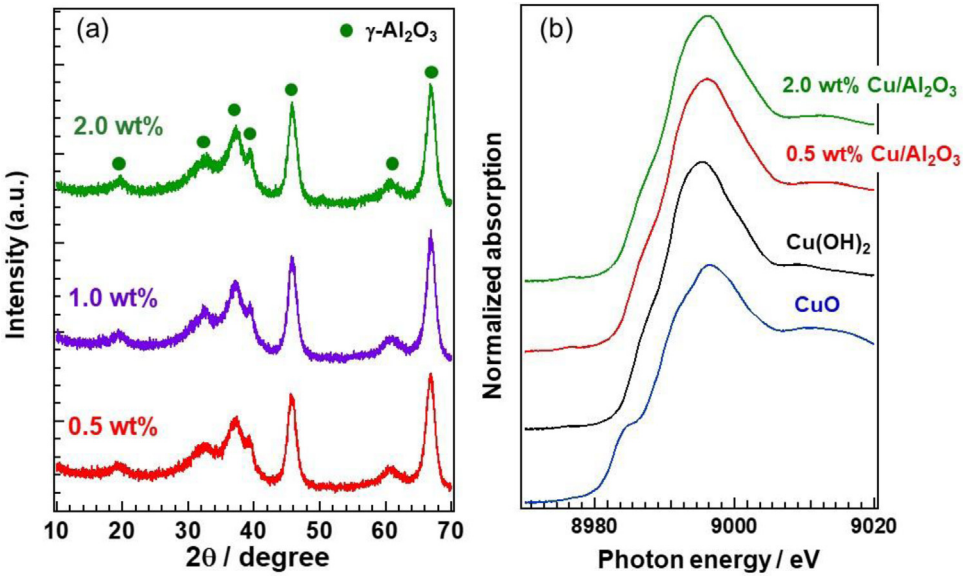

Fig. 1. (a) XRD patterns and (b) Cu K-edge XANES spectra of Cu/Al_2O_3 with various amounts of Cu loading.

lowed by calcination at 773 K. XRD patterns of Cu/Al_2O_3 catalysts with various loading amounts of Cu were acquired (Fig. 1(a)). Unfortunately, the peaks associated with the Cu species were undetectable even for the 2.0 wt% Cu/Al_2O_3 sample. Then, the Cu K-edge X-ray absorption near edge structure (XANES) spectrum of 0.5 wt% Cu/Al_2O_3 is almost identical to that of the 2.0 wt% Cu/Al_2O_3 sample (Fig. 1(b)). The features of these spectra are close to those of $Cu(OH)_2$ that contains an octahedral Cu^{2+} species. The extended X-ray absorption fine structure (EXAFS) oscillation of 0.5 wt% Cu/Al_2O_3 is essentially identical to that of 2.0 wt% Cu/Al_2O_3 (Fig. S1(a)). In the Fourier-transform of EXAFS spectra, no peak at 2–4 Å, corresponding to Cu–Cu bonds, was observed even in 2.0 wt% Cu/Al_2O_3 (Fig. S1(b)). These results indicate that octahedral Cu^{2+} species are highly dispersed on Al_2O_3, even at 2.0 wt% loading.

To investigate the dispersion state of Cu^{2+} species on γ-Al_2O_3 in detail, we investigate Cu/Al_2O_3 catalysts by using ESR spectra, in which Cu^{2+} (d^9) species showing paramagnetic resonance is well-known to be detectable for a highly-dispersed Cu^{2+} species on supports [38–40]. Axially symmetric signals originating from the copper nuclear spin of 1/2 were observed for the Cu/Al_2O_3 catalysts examined in this work (Fig. 2); in other words, Cu/Al_2O_3 catalysts have a parallel component ($g_{//}$ = 2.33) and a perpendicular component ($g\perp$ = 2.05). As was previously reported by us and other groups [38–40], the 0.1 and 0.5 wt% Cu/Al_2O_3 samples clearly exhibit parallel hyperfine components that are divided into four signals, while these hyperfine structures become obscured for catalysts having Cu loadings above 1.0 wt%. A signal ($g_{//}$ = 2.23) influenced by neighboring Cu^{2+} species clearly appears in the 1.0 wt% and 2.0 wt% Cu/Al_2O_3 sample. The parallel hyperfine components, which are due to isolated Cu^{2+} species, are known to be generally broadened by magnetic dipole-dipole interactions with neighboring Cu^{2+} species. In other words, the distance between Cu^{2+} species highly dispersed on Al_2O_3 is suggested to approach by increasing Cu loading. Therefore, we conclude that 0.1 and 0.5 wt% Cu/Al_2O_3 contain only isolated Cu^{2+} species, and that local aggregation of Cu species begins around 1.0 wt% Cu loading.

Since an aggregated Cu^{2+} solid species is scarcely detectable by ESR techniques, the peak intensities associated with Cu loading actually decrease for catalysts with high Cu loadings. In addition, the ESR spectrum of 0.5 wt% Cu catalysts supported on CeO_2 or ZrO_2 hardly shows any parallel hyperfine component arising from isolated Cu species (Fig. S2), suggesting that the Al_2O_3 support assists in the formation of the isolated Cu^{2+} species.

Table 1
Results for deconvoluted peaks in Al K-edge XANES spectra.

	Relative ratio of the peak areas (%)		
	Peak at 1565 eV[a]	Peak at 1568 eV[b]	Peak at 1570 eV[b]
γ-Al_2O_3	43	14	43
0.5 wt% Cu/γ-Al_2O_3	27	25	48

[a] The peak was attributed to tetrahedral Al species.
[b] The peaks were attributed to distorted octahedral Al species.

The Al_2O_3 used in this study is γ-Al_2O_3, which has a spinel structure consisting of both tetrahedral and octahedral Al species (Fig. 3(a)). The relative ratio of tetrahedral to octahedral Al sites is known to alter through the introduction of defects [41]. The XANES spectrum of the Al K-edge of γ-Al_2O_3 sample is shown in Fig. 3(b). The observed peaks are due to electronic transitions from 1 s to 3p orbitals. Spectra of $LaAlO_3$, α-Al_2O_3 and $AlPO_4$ are shown as reference. $LaAlO_3$ and α-Al_2O_3 contain distorted octahedral Al species, while $AlPO_4$ is only composed of tetrahedral Al species. On the basis of these reference spectra and previous reports [42,43], the peak at 1565 eV is assigned to tetrahedral Al species, and the peaks at 1568 eV and 1570 eV to distorted octahedral Al species; in other words, γ-Al_2O_3 exhibits peaks belonging to both tetrahedral and octahedral Al species. In the Al K-edge XANES spectrum of the 0.5 wt% Cu/Al_2O_3 catalyst, Cu loading diminishes the peak at around 1565 eV belonging to the tetrahedral species. Then, the relative ratio of tetrahedral Al species was estimated by a fitting analysis with Al K-edge XANES spectrum (Fig. S3). The peak area due to tetrahedral Al species clearly decreased by Cu loading (Table 1), suggesting that the tetrahedral Al species must be transformed to octahedral Al species by the interaction between Cu species and the tetrahedral Al species in Al_2O_3. These results allow us to conclude that the isolated Cu^{2+} species in 0.5 wt% Cu/Al_2O_3 is formed by interacting with tetrahedral Al species in γ-Al_2O_3.

3.2. Selective reduction of NO over Cu/Al_2O_3 catalysts

Fig. 4(a and b) shows the results of the reactions of NO-CO-C_3H_6 at 773 K over 0.5 wt% and 2.0 wt% Cu/Al_2O_3 catalysts under various oxygen concentration conditions. The catalytic activities for

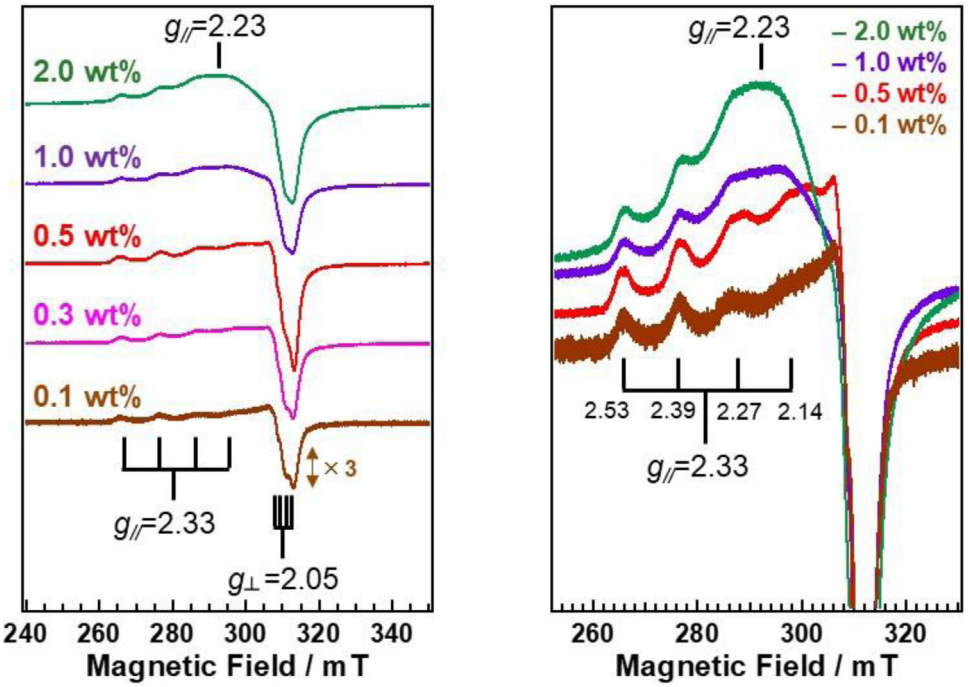

Fig. 2. ESR spectra of Cu/Al_2O_3 with various amounts of Cu loading.

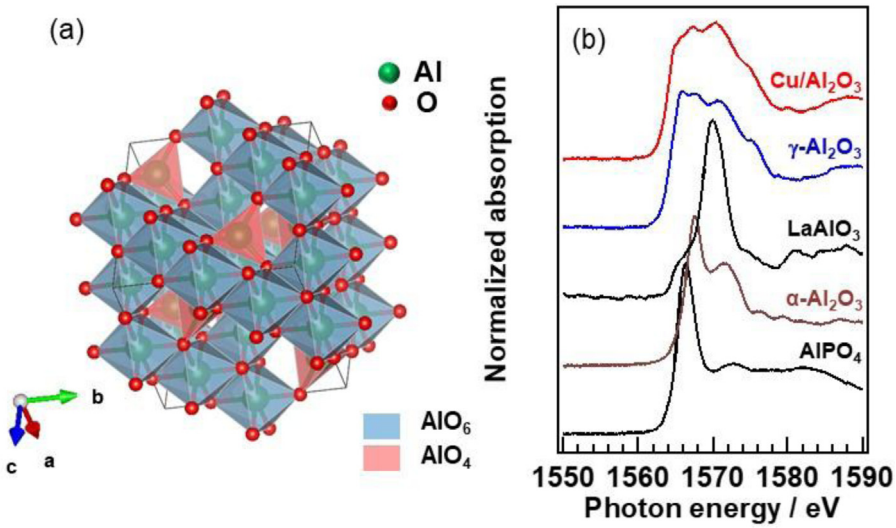

Fig. 3. (a) Crystal structure of γ-Al_2O_3. (b) Al K-edge XANES spectra of Al_2O_3, 0.5 wt% Cu/Al_2O_3, and reference samples.

NO reduction over the Cu/Al_2O_3 catalysts, with controlled amounts of Cu loading, were superior to that of Pd/Al_2O_3 under lean ($\lambda > 1$) and rich ($\lambda < 1$) conditions, but under stoichiometric oxygen condition ($\lambda = 1$); 0.5 wt% Pd/Al_2O_3 effectively reduced NO to N_2 only under stoichiometric oxygen condition. Specifically, the 0.5 wt% Cu/Al_2O_3 catalyst showed high catalytic activity under lean conditions ($1.2 < \lambda < 1.79$), and the 2.0 wt% Cu/Al_2O_3 was effective under rich conditions ($0.47 < \lambda < 1.0$). CeO_2 or ZrO_2-supported 0.5 wt% Cu catalyst exhibited high catalytic activity only under stoichiometric and/or rich conditions (Fig. 4(c and d)), while NO reduction on these catalysts hardly proceeded under lean conditions. No N_2O formation was observed on Cu-based catalysts (Fig. S4), while Pd/Al_2O_3 catalyst slightly reduced NO to N_2O under lean conditions ($\lambda = 1.26–1.05$). Considering the difficulty in achieving NO reduction under lean conditions over Pd/Al_2O_3 or supported Cu catalysts, the efficient reduction of NO under lean conditions ($\lambda > 1$) using the 0.5 wt% Cu/Al_2O_3 catalyst is very interesting.

The catalytic activities for CO and C_3H_6 oxidation, over the catalysts examined in this study, increase with increasing oxygen concentration. With the exception of 0.5 wt% Cu/Al_2O_3, these pollutants were completely oxidized to CO_2 under conditions in which the oxygen concentrations were more than stoichiometric condition ($\lambda = 1$). On the other hand, the residual C_3H_6 or CO was observed in the reactions under the lean conditions over 0.5 wt% Cu/Al_2O_3 catalyst.

The catalytic activities of the NO-CO-O_2 and NO-C_3H_6-O_2 reactions over 0.5 wt% Cu/Al_2O_3 were also investigated (Fig. S5). NO reduction in the presence of only CO hardly proceeds on 0.5 wt% Cu/Al_2O_3, while the analogous reduction with C_3H_6 showed high catalytic activity even under lean conditions. The catalytic activity

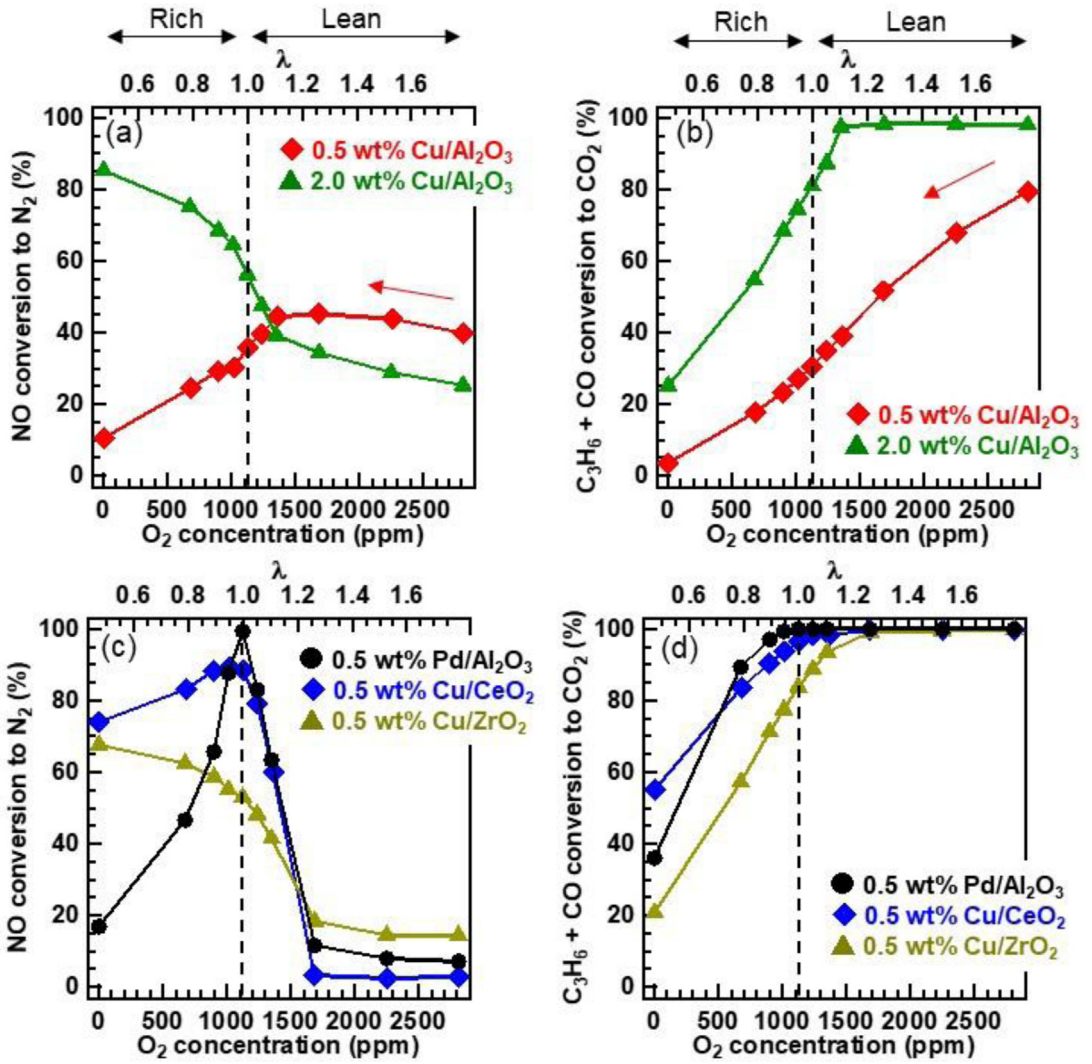

Fig. 4. Selective reductions of NO under a variety of oxygen concentrations at 773 K; (a) and (c) conversion of NO to N_2; (b) and (d) conversion of C_3H_6 + CO to CO_2. The reaction gas (100 mL min^{-1}), composed of 1000 ppm NO, 1000 ppm CO, 250 ppm C_3H_6, 2812.5–0 ppm O_2, and He as the balance, was introduced to the catalyst bed. The concentrations of CO, C_3H_6 and NO were fixed, and [O_2] varied from 2812.5 ppm to 0 ppm. The oxygen concentration at a stoichiometric condition (λ = 1) is 1125 ppm.

with C_3H_6 alone is comparable to that with C_3H_6 and CO under lean conditions, suggesting that C_3H_6 is mainly used as a reductant for the NO-CO-C_3H_6 reaction in the presence of O_2 over 0.5 wt% Cu/Al_2O_3.

The effect of Cu loading on the Al_2O_3-supported catalyst, for NO reduction activity under various oxygen concentrations at 773 K, was investigated (Fig. 5). Increases in Cu loading under rich or stoichiometric conditions resulted in enhanced NO reduction activity. However, under lean conditions, the 0.5 wt% Cu/Al_2O_3 catalyst exhibited the highest NO reduction activity among the examined Cu/Al_2O_3 catalysts.

Based on the characterization and the reaction results of Cu/Al_2O_3 catalysts with various Cu loading amounts, the oxidation characteristics of isolated Cu^{2+} species strongly interacted with tetrahedral Al species is much inferior to that of bulk Cu species. Accordingly, we conclude that NO reduction on 0.5 wt% Cu/Al_2O_3 proceeds by utilizing the residual CO and C_3H_6 even in lean conditions.

3.3. *Precious-group-metal loaded Cu/Al_2O_3 catalysts*

An infinitesimal loading (0.01 wt%, 100 ppm) of precious metal on 0.5 wt% Cu/Al_2O_3 dramatically influenced its catalytic activity. Fig. 6(a and b) shows the results of NO-CO-C_3H_6 reactions at 773 K under various oxygen concentrations over 0.01 wt% PGM/Cu/Al_2O_3 catalysts. For CO_2 production derived from CO and C_3H_6 combustion under lean conditions, all of these modified catalysts exhibit much higher activities than Cu/Al_2O_3 alone. $Pt/Cu/Al_2O_3$ and $Pd/Cu/Al_2O_3$ showed high catalytic activities for NO reduction only under stoichiometric condition, and formed a small amount of N_2O under slightly lean conditions (λ = 1.26–1.05) (Fig. S6). Interestingly, NO reduction on $Rh/Cu/Al_2O_3$ effectively proceeded without N_2O formation over the entire oxygen concentration range, although Cu/Al_2O_3 itself showed low catalytic activity under stoichiometric and rich conditions.

The Rh/Al_2O_3 catalysts hardly showed any NO reduction activity under lean conditions regardless of Rh loading amount (Fig. 6(c and d)). $Rh/Cu/Al_2O_3$ had high oxidation activity under lean conditions with maintaining the high NO reduction activity of Cu/Al_2O_3 itself, although the oxidation activity of Cu/Al_2O_3 did not reach 100%. NO reduction under around stoichiometric conditions proceeded poorly on 0.01 wt% Rh/Al_2O_3, while Rh loaded on Cu/Al_2O_3 proceeded to completely reduce NO. Actually, for selective reduction of NO under stoichiometric condition (Fig. 7), $Rh/Cu/Al_2O_3$ displayed much higher catalytic activity at lower temperatures than 0.01 wt% Rh/Al_2O_3 or 0.5 wt% Cu/Al_2O_3 itself, suggesting that a synergistic

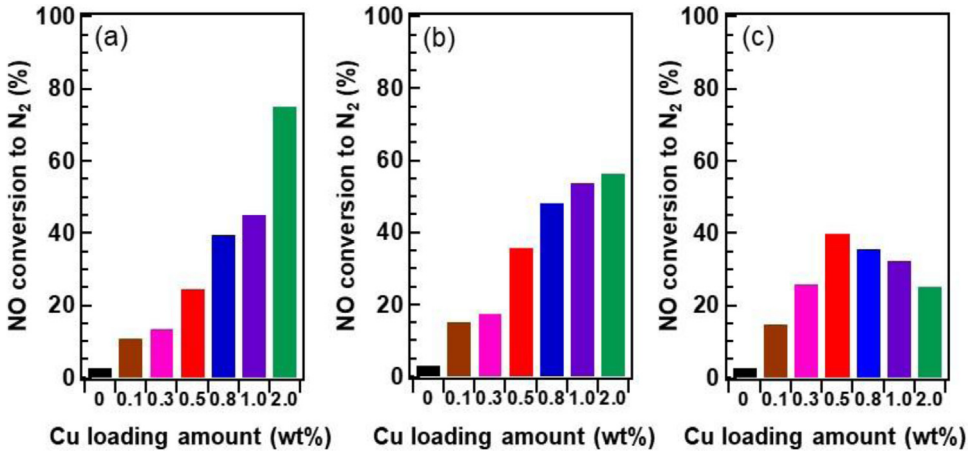

Fig. 5. Effect of Cu loading on N_2 production under a variety of oxygen concentrations. (a) Low oxygen concentration (λ = 0.79); (b) stoichiometric condition (λ = 1.00); (c) high oxygen concentration (λ = 1.79).

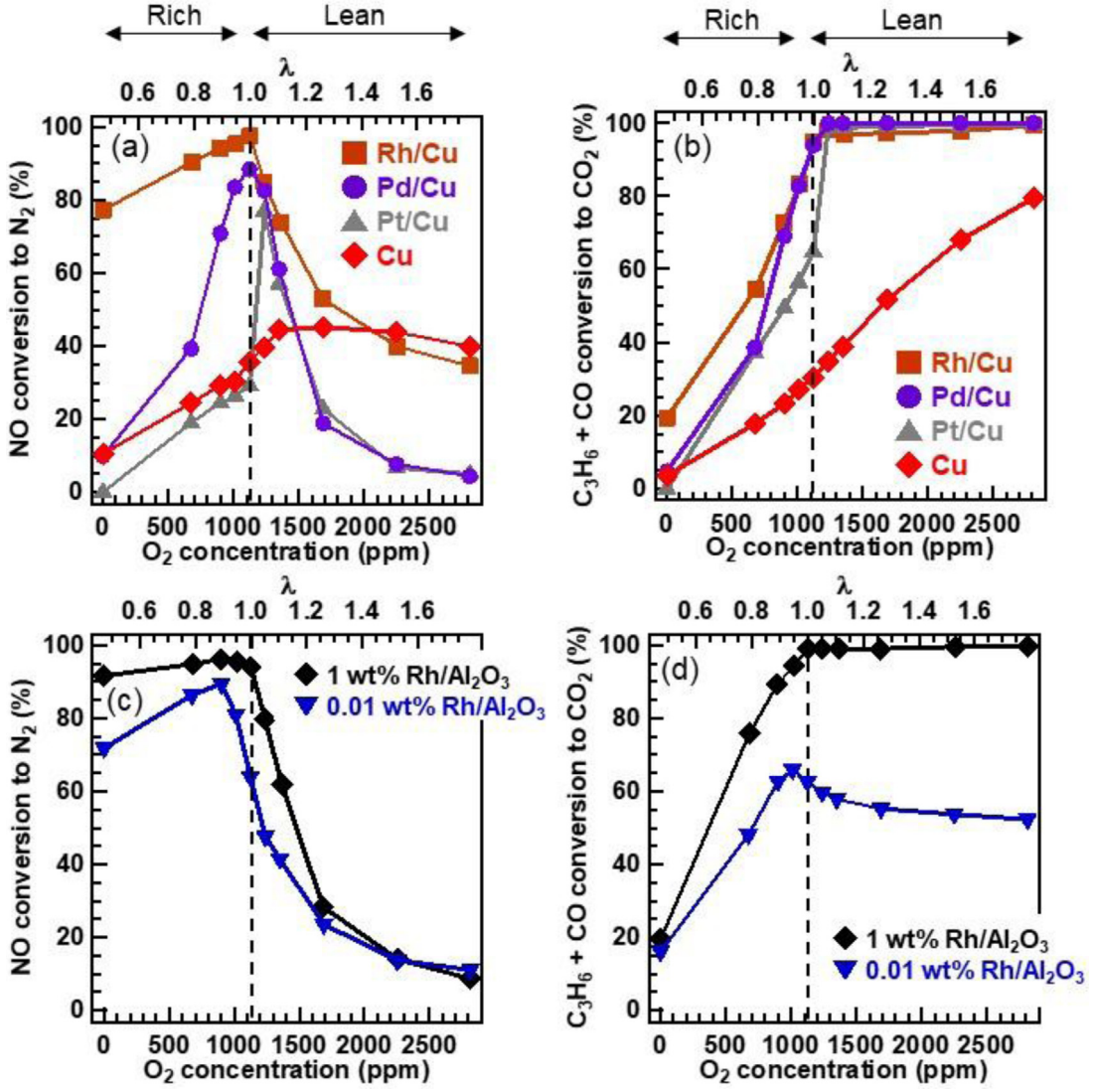

Fig. 6. Selective reductions of NO under a variety of oxygen concentrations on 0.01 wt% PGM/0.5 wt% Cu/Al_2O_3 (PGM/Cu) and Rh/Al_2O_3; (a) and (c) conversion of NO to N_2; (b) and (d) conversion of C_3H_6 + CO to CO_2.

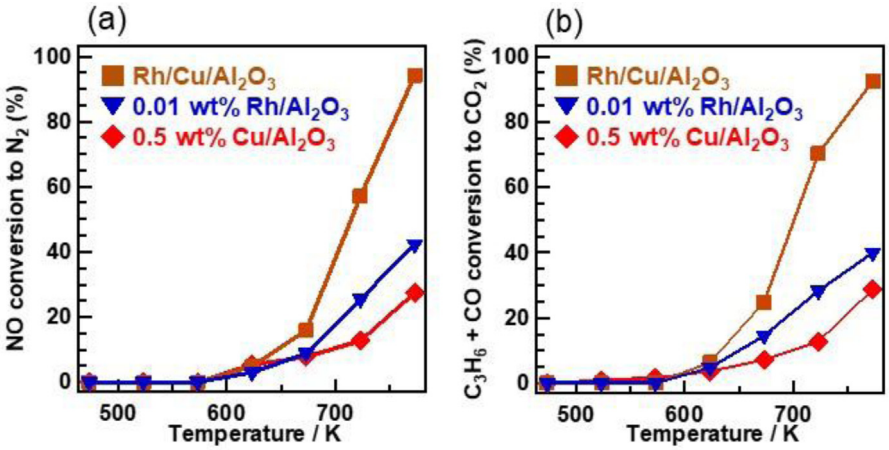

Fig. 7. Selective reductions of NO under stoichiometric condition over 0.01 wt% Rh/0.5 wt% Cu/Al_2O_3; (a) conversion of NO to N_2; (b) conversion of C_3H_6 + CO to CO_2.

effect operates as a result of Rh loading onto Cu/Al_2O_3 under stoichiometric condition. Clearly, an infinitesimal amount of Rh loaded on 0.5 wt% Cu/Al_2O_3 provides the following effects: (1) The oxidation activity under lean conditions using Cu/Al_2O_3 is improved by Rh loading, while the high reduction activity of Cu/Al_2O_3 is maintained; and (2) catalytic activities under rich and stoichiometric conditions over Cu/Al_2O_3 are dramatically enhanced.

The optimal Rh loading amount was investigated (Fig. S7). The catalytic activities under the rich and stoichiometric conditions of 0.5 wt% Cu/Al_2O_3 itself were drastically improved even by 0.005 wt% Rh loading, while NO reduction under the stoichiometric condition was inadequate. The catalytic activities under the entire oxygen concentrations of 0.02 wt% $Rh/Cu/Al_2O_3$ were essentially identical with those of 0.01 wt% $Rh/Cu/Al_2O_3$; however, the catalytic activities under lean conditions of the former catalyst slightly decreased compared to those of the latter catalyst. One of the reasons is that the excessively-loaded Rh species must inhibit the role of 0.5 wt% Cu/Al_2O_3. From these results, the optimal Rh loading amount for 0.5 wt% Cu/Al_2O_3 is determined to be 0.01 wt%, 100 ppm. Thus, we reveal that Rh-loaded Cu/Al_2O_3 catalyst can effectively share the role of Rh and Cu species by an infinitesimal loading of Rh.

To confirm the state of Cu species in 0.01 wt% Rh/0.5 wt% Cu/Al_2O_3, we carried out XPS and ESR measurements (Fig. S8). The Cu 2p spectrum of $Rh/Cu/Al_2O_3$ is essentially identical with that of Cu/Al_2O_3. Interestingly, ESR analysis reveals that parallel hyperfine components observed in 0.5 wt% Cu/Al_2O_3 become a little unclear by Rh loading, suggesting that the aggregation of isolated Cu^{2+} species slightly proceeds by Rh loading. However, since the majority of Cu species in $Rh/Cu/Al_2O_3$ is preserved as the isolated Cu^{2+} species regardless of the Rh loading, $Rh/Cu/Al_2O_3$ maintains the high catalytic activity under lean condition of Cu/Al_2O_3 itself.

Fig. 8 displays the DRIFT spectra of adsorbed species during NO-C_3H_6-O_2 reactions at 773 K under high oxygen concentration condition (lean condition) over 0.01 wt% PGM/0.5 wt% Cu/Al_2O_3. The Cu/Al_2O_3 sample displays bands at around 2116 cm^{-1} and 2151 cm^{-1}, which are assigned to Cu^+-CO and nitrile species, respectively [44–46]. In addition, Cu/Al_2O_3 displays a weak band at 2232 cm^{-1} assigned to NCO species bound to Al ions (Al-NCO). These species are clearly observed on the $Rh/Cu/Al_2O_3$ catalyst, even under lean conditions, compared to $Pd/Cu/Al_2O_3$. The formation of N_2 during the selective reductions has been reported to occur via intermediates such as isocyanates and nitriles [46]. These results reveal that small amounts of loaded Pd inhibit the formation of intermediates such as isocyanates and nitriles on Cu/Al_2O_3 under lean conditions, resulting in low catalytic activity for NO reduction

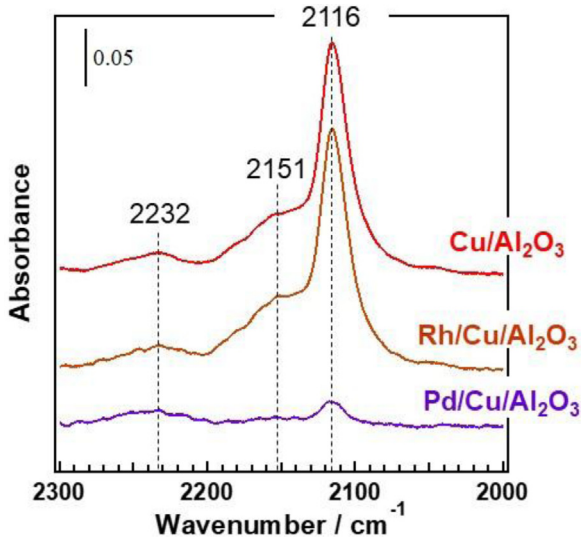

Fig. 8. DRIFT spectra at 773 K under NO-C_3H_6-O_2 flow corresponding to a lean condition. The reaction gas condition is as follows: total flow rate, 100 mL min^{-1}; NO, 1000 ppm; C_3H_6, 250 ppm; O_2, 2250 ppm; He balance.

under these conditions. On the other hand, even under lean conditions, these intermediates are still observed for $Rh/Cu/Al_2O_3$. These results demonstrate that the catalytic activity of Cu/Al_2O_3 itself is preserved under lean conditions, regardless of Rh loading.

Inspired by the results obtained from DRIFT spectroscopy, the oxidation activities of $Pd/Cu/Al_2O_3$, $Rh/Cu/Al_2O_3$ and 0.5 wt% Cu/Al_2O_3 toward CO or C_3H_6 combustion were investigated (Fig. 9). An infinitesimal loading of Pd dramatically enhanced the oxidation activity of Cu/Al_2O_3. As expected, there was no significant improvement in the combustion activity of Rh-loaded Cu/Al_2O_3. These results suggest that Rh loading hardly promotes CO and C_3H_6 combustion compared to Pd loading. Considering the DRIFT result and the oxidation activity of $Rh/Cu/Al_2O_3$, one of the synergetic effects of Rh and Cu species is the moderate improvement of oxidation characteristics for 0.5 wt% Cu/Al_2O_3 itself. As shown in Fig. 6, $Rh/Cu/Al_2O_3$ shows the higher oxidation activity under lean condition ($\lambda = 1.79$) than 0.01 wt% Rh/Al_2O_3 or 0.5 wt% Cu/Al_2O_3 itself. The CO conversions (69%) on 0.5 wt% Cu/Al_2O_3 was essentially identical with that (61%) on 0.01 wt% Rh/Al_2O_3. Interestingly, C_3H_6 conversion on 0.5 wt% Cu/Al_2O_3 reached 100%, while 0.01 wt% Rh/Al_2O_3 remained C_3H_6 (Conv. = 41%) even under the lean condition. Therefore, in the case of 0.01 wt% Rh/0.5 wt% Cu/Al_2O_3,

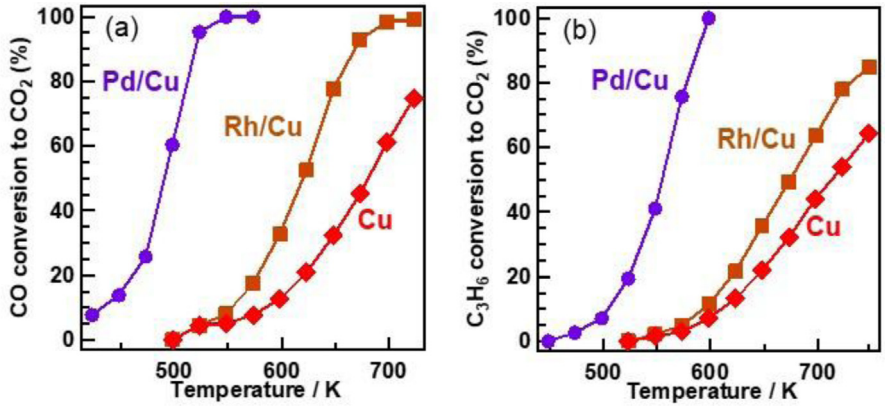

Fig. 9. Combustion data as functions of temperature. (a) CO and (b) C_3H_6 combustion over 0.5 wt% Cu/Al_2O_3 (Cu), and 0.01 wt% PGM/0.5 wt% Cu/Al_2O_3 (PGM/Cu).

Rh species moderately helps the oxidation characteristics of Cu species, resulting in the enhancement for CO and C_3H_6 oxidation under lean condition with maintaining the high NO reduction activity of Cu/Al_2O_3 itself. Unfortunately, since the loading of Pd species having extremely-high oxidation characteristics inhibits the formation of isocyanates and nitriles over Cu/Al_2O_3, $Pd/Cu/Al_2O_3$ hardly shows the catalytic activity for NO reduction under lean condition.

4. Conclusions

Catalytic NO-CO-C_3H_6-O_2 reactions over Cu/Al_2O_3 are significantly influenced by the amount of Cu loading. As Cu loading is increased, the catalytic activities under rich and stoichiometric conditions increase. In contrast, 0.5 wt% Cu/Al_2O_3 showed the highest activity under lean conditions among the examined catalysts, and the catalytic activity is significantly superior to that of the PGM catalyst, Pd/Al_2O_3. ESR and XAFS spectra reveal that an isolated Cu^{2+} species, which strongly interacts with the tetrahedral Al species in γ-Al_2O_3, plays a role as an active site under lean conditions. In addition, this study demonstrates the following unambiguous facts in relation to the effects of an infinitesimal amount (0.01 wt%, 100 ppm) of Rh loaded onto Cu/Al_2O_3. Rh loading on 0.5 wt% Cu/Al_2O_3 shows high catalytic activity over the entire oxygen concentration range, although the catalytic activity of 0.5 wt% Cu/Al_2O_3 alone is low under stoichiometric or rich condition. On the other hand, Pt or Pd loading diminishes NO reduction activity under lean conditions. DRIFT spectra indicate that $Rh/Cu/Al_2O_3$ forms isocyanates and nitriles under lean conditions, which are intermediates in these selective reductions of NO. Since $Pd/Cu/Al_2O_3$ has extremely high oxidation activity, no such intermediate species are detected under lean conditions using this catalyst. These results suggest that NO reduction on $Rh/Cu/Al_2O_3$ proceeds through the intermediates formed from CO and/or C_3H_6, even under lean conditions. Therefore, the infinitesimal loading of Rh on Cu/Al_2O_3 enables us to effectively share the roles of Cu species and Rh species according to oxygen concentration in NO-CO-C_3H_6 reaction. These observations provide the novel guideline for the development of catalysts that more beneficially use precious metal resources.

Acknowledgements

This work was partially supported by the Program for Elements Strategy Initiative for Catalysts & Batteries (ESICB) and by a Grant-in-Aid for Scientific Research (B) (General) (16H04567). The X-ray absorption experiments were performed with the approval of the Japan Synchrotron Radiation Research Institute (JASRI) and the Institute for Molecular Science (Proposal No. 2014B1371 and No. 14-801).

Appendix A. Supplementary data

Supplementary data associated with this article can be found, in the online version, at http://dx.doi.org/10.1016/j.mcat.2017.09.005.

References

[1] A. Fritz, V. Pitchon, Appl. Catal. B: Environ. 13 (1997) 1–25.
[2] M.V. Twigg, Catal. Today 163 (2011) 33–41.
[3] M. Haneda, H. Hamada, CR Chim. 19 (2016) 1254–1265.
[4] J. Kašpar, P. Fornasiero, M. Graziani, Catal. Today 50 (1999) 285–298.
[5] H. He, H.X. Dai, L.H. Ng, K.W. Wong, C.T. Au, J. Catal. 206 (2002) 1–13.
[6] P. Bera, K.C. Patil, V. Jayaram, G.N. Subbanna, M.S. Hegde, J. Catal. 196 (2000) 293–301.
[7] H. Hamada, M. Haneda, Appl. Catal. A: Gen. 421–422 (2012) 1–13.
[8] S. Misumi, H. Yoshida, S. Hinokuma, T. Sato, M. Machida, Sci. Rep. 6 (2016) 29737.
[9] K. Sato, T. Yoshinari, Y. Kintaichi, M. Haneda, H. Hamada, Appl. Catal. B: Environ. 44 (2003) 67–78.
[10] J. Wang, H. Chen, Z. Hu, M. Yao, Y. Li, Catal. Rev. 57 (2015) 79–144.
[11] H. Tanaka, Catal. Surv. Asia 9 (2005) 63–74.
[12] K. Sato, H. Tomonaga, T. Yamamoto, S. Matsumura, N.D. Zulkifli, T. Ishimoto, M. Koyama, K. Kusada, H. Kobayashi, H. Kitagawa, K. Nagaoka, Sci. Rep. 6 (2016) 28265.
[13] H. Hamada, Catal. Today 22 (1994) 21–40.
[14] H. Yoshida, Y. Okabe, N. Yamashita, S. Hinokuma, M. Machida, Catal. Today 281 (2017) 590–595.
[15] M.D. Amiridis, T. Zhang, R.J. Farrauto, Appl. Catal. B: Environ. 10 (1996) 203–227.
[16] M. Iwamoto, H. Hamada, Catal. Today 10 (1991) 57–71.
[17] Q. Yu, X. Wu, X. Yao, B. Liu, F. Gao, J. Wang, L. Dong, Catal. Commun. 12 (2011) 1311–1317.
[18] P.M. Sreekanth, P.G. Smirniotis, Catal. Lett. 122 (2007) 37–42.
[19] D. Stoyanovaa, M. Christovaa, P. Dimitrovaa, J. Marinovab, N. Kasabovab, D. Panayotova, Appl. Catal. B: Environ. 17 (1998) 233–244.
[20] K. Ueda, C.A. Ang, Y. Ito, J. Ohyama, A. Satsuma, Catal. Sci. Technol. 6 (2016) 5797–5800.
[21] P. Granger, V.I. Parvulescu, Chem. Rev. 111 (2011) 3155–3207.
[22] Y. Nagao, Y. Nakahara, T. Sato, H. Iwakura, S. Takeshita, S. Minami, H. Yoshida, M. Machida, ACS Catal. 5 (2015) 1986–1994.
[23] J. Kašpar, P. Fornasiero, N. Hickey, Catal.Today 77 (2003) 419–449.
[24] J.H. Kwak, R. Tonkyn, D. Tran, D. Mei, S.J. Cho, L. Kovarik, J.H. Lee, C.H.F. Peden, J. Szanyi, ACS Catal. 2 (2012) 1432–1440.
[25] P.A. Kumar, M.P. Reddy, L.K. Ju, B. Hyun-Sook, H.H. Phil, J. Mol. Catal. A: Chem. 291 (2008) 66–74.
[26] Y. Hu, L. Dong, M. Shen, D. Liu, J. Wang, W. Ding, Y. Chen, Appl. Catal. B: Environ. 31 (2001) 61–69.
[27] S.D. Peter, E. Garbowski, V. Perrichon, B. Pommier, M. Primet, Appl. Catal. A: Gen. 205 (2001) 147–158.
[28] A. Martínez-Arias, A.B. Hungría, A. Iglesias-Juez, M. Fernández-García, J.A. Anderson, J.C. Conesa, G. Munuera, J. Soria, Catal. Today 180 (2012) 81–87.
[29] L. Liu, J. Cai, L. Qi, Q. Yu, K. Sun, B. Liu, F. Gao, L. Dong, Y. Chen, J. Mol. Catal. A: Chem. 327 (2010) 1–11.
[30] J.D.A. Bellido, E.M. Assaf, Fuel 88 (2009) 1673–1679.

[31] M. Iwamoto, H. Furukawa, Y. Mine, F. Uemura, S. Mikuriya, S. Kagawa, J. Chem. Soc. Chem. Commun. (1986) 1272–1273.
[32] J. Xiaoyuan, L. Lipining, C. Yingxu, Z. Xiaoming, J. Mol. Catal. A: Chem. 197 (2003) 193–205.
[33] J.N. Armor, Catal. Today 31 (1996) 191–198.
[34] H. Yahiro, M. Iwamoto, Appl. Catal. A: Gen. 222 (2001) 163–181.
[35] K. Shimizu, H. Maeshima, A. Satsuma, T. Hattori, Appl. Catal. B: Environ. 18 (1998) 163–170.
[36] T. Ohnishi, K. Kawakami, M. Nishioka, M. Ogura, Catal. Today 281 (2017) 566–574.
[37] T. Yamamoto, T. Tanaka, R. Kuma, S. Suzuki, F. Amano, Y. Shimooka, Y. Kohno, T. Funabiki, S. Yoshida, Phys. Chem. Phys. Chem. 4 (2002) 2449–2458.
[38] F. Amano, S. Suzuki, T. Yamamoto, T. Tanaka, Appl. Catal. B: Environ. 64 (2006) 282–289.
[39] A. Martínez-Arias, R. Cataluña, J.C. Conesa, J. Soria, J. Phys. Chem. B 102 (1998) 809–817.
[40] F. Amano, T. Tanaka, T. Funabiki, J. Mol. Catal. A: Chem. 221 (2004) 89–95.
[41] G. Gutiérrez, A. Taga, B. Johansson, Phys. Rev. B 65 (2001) 012101.
[42] D. Li, G.M. Bancroft, M.E. Fleet, X.H. Feng, Y. Pan, Am. Min. 80 (1995) 432–440.
[43] D.R. Neuville, L. Cormier, D. Massiot, Geochim. Comoschim. Acta 68 (2004) 5071–5079.
[44] K. Shimizu, H. Kawabata, H. Maeshima, A. Satsuma, T. Hattori, J. Phys. Chem. B 104 (2000) 2885–2893.
[45] A. Dandekar, M.A. Vannice, J. Catal. 178 (1998) 621–639.
[46] J. Liu, X. Li, Q. Zhao, C. Hao, D. Zhang, Environ. Sci. Technol. 47 (2013) 4528–4535.